J|A|C|S ARTICLES

Published on Web 08/23/2010

Synthesis, Reactions, and Electronic Properties of 16 π-Electron Octaisobutyltetraphenylporphyrin

Yohsuke Yamamoto,*[,†] Yusuke Hirata,[†] Megumi Kodama,[†] Torahiko Yamaguchi,[†] Shiro Matsukawa,[†,○] Kin-ya Akiba,[‡] Daisuke Hashizume,[§] Fujiko Iwasaki,[⊥] Atsuya Muranaka,[||] Masanobu Uchiyama,[||,∞] Ping Chen,[#] Karl M. Kadish,[#] and Nagao Kobayashi[▽]

Department of Chemistry, Graduate School of Science, Hiroshima University, 1-3-1 Kagamiyama, Higashi-Hiroshima 739-8526, Japan, Advanced Research Center for Science and Engineering, Waseda University, 3-4-1 Ohkubo, Shinjuku-ku, Tokyo 169-8555, Japan, Molecular Characterization Team and Advanced Elements Chemistry Laboratory, Institute of Physics and Chemistry Research, RIKEN, 2-1 Hirosawa, Wako, Saitama 351-0198, Japan, X-ray Laboratory, Rigaku Corporation, 3-9-12, Matsubaracho, Akishima, Tokyo 195-8666, Japan, Department of Chemistry, University of Houston, Houston, Texas 77204-5003, and Department of Chemistry, Graduate School of Science, Tohoku University, Aoba-ku, Miyagi 980-8578, Japan

Received April 11, 2010; E-mail: yyama@sci.hiroshima-u.ac.jp

Abstract: The reaction of the doubly oxidized β-octaisobutyl-*meso*-tetraphenylporphyrin (OiBTPP, **4**), which has a 16 π-electronic structure at the porphyrin core, with a variety of metal reagents was investigated. The reaction of **4** with $SnCl_2$ followed by ethanolysis afforded an 18 π-electron tin complex, (OiBTPP)-$Sn(OEt)_2$ (**5**), in a redox manner. No reactions were observed using zerovalent metals (Zn, Cu, and Pd). However, the reaction of 16π $[(OiBTPP)Li]^+[BF_4]^-$ (**6**), which was easily derived from **4**, with Zn, Cu, and $Pd_2(dba)_3$ gave the corresponding 18π metalloporphyrins (OiBTPP)M (**7**, M = Zn(EtOH); **8**, M = Cu; and **9**, M = Pd). One-electron oxidation of the copper complex **8** by $AgSbF_6$ afforded a 17 π-electron cation radical complex, $[(OiBTPP)Cu]^{\bullet+}[SbF_6]^-$ (**10**). The UV−visible and electron spin resonance spectra of **10** were quite similar to those of previously reported β-octaethyl-*meso*-tetraphenylporphyrin (OETPP) derivatives, $[(OETPP)Cu]^{\bullet+}X^-$ (X = ClO_4, I). In contrast to the reaction of **6** with Zn to give the 18π complex **7**, the reaction of **4** with divalent $ZnCl_2$ enabled us to isolate a new 16π porphyrin−zinc(II) complex, $[(OiBTPP)Zn(Cl)]^+[ZnCl_3]^-$ (**11**), in 92% yield. The solid-state structures of **5** and **7**−**11** were unambiguously determined by single-crystal X-ray crystallography. The porphyrin cores of **10** (17π) and **11** (16π) are much more distorted than those of the 18π derivatives **5** and **7**−**9**. Furthermore, the bond distances of **10** and **11** clearly showed the presence of bond alternation in contrast to aromatic 18π species **8** and **7**, respectively. Nucleus-independent chemical shift calculations of **4** and some metalated porphyrins indicated that the highly distorted 16π porphyrins are essentially nonaromatic, with only weak antiaromaticity. Magnetic circular dichroism studies in conjunction with ZINDO/S calculations assisted in identifying the electronic transitions of the UV−vis spectra of key porphyrins. Electrochemical and thin-layer UV−vis spectroelectrochemical experiments on **4** (16π) and **11** (16π) indicated that both compounds can be electroreduced to give the 18π species, with the 16π/18π transition being reversible in the case of $[(OiBTPP)Zn(Cl)]^+[ZnCl_3]^-$ (**11**).

Introduction

Porphyrins, macrocycles having four pyrrole rings connected with four methine carbons, have drawn much attention through the years due to their close relevance to biological activities involving heme proteins.[1] Thus, a number of studies on porphyrin derivatives, especially metalloporphyrins, have been carried out, and through these endeavors unique structural, photochemical, and electrochemical characters have been revealed.[2]

Ordinary porphyrins have an aromatic 18 π-electron conjugated system delocalized over 24 core atoms, satisfying Hückel's $(4n + 2)$ π-electron rule. As for 4*n* π-electron porphyrins, they could in principle be obtained by the oxidation or reduction of the 18π system (Scheme 1). However, due to their unstable

[†] Hiroshima University.
[‡] Waseda University.
[§] Molecular Characterization Team, RIKEN.
[||] Advanced Elements Chemistry Lab, RIKEN.
[⊥] Rigaku Corp.
[#] University of Houston.
[▽] Tohoku University.
[○] Current address: Department of Chemistry, Faculty of Science, Toho University, Funabashi 274-8510, Japan.
[∞] Current address: Graduate School of Pharmaceutical Sciences, The University of Tokyo, 7-3-1 Hongo, Bunkyo-ku, Tokyo 113-0033, Japan.

(1) (a) Mansuy, D.; Battioni, P. In *The Porphyrin Handbook*; Kadish, K. M., Smith, K. M., Guilard, R., Eds.; Academic Press: Burlington, MA, 2000, Vol. 4, pp 1−15. (b) Poulos, T. In *The Porphyrin Handbook*; Kadish, K. M., Smith, K. M., Guilard, R., Eds.; Academic Press: Burlington, MA, 2000, Vol. 4, pp 189−218. (c) Ogoshi, H.; Mizutani, T.; Hayashi, T.; Kuroda, Y. In *The Porphyrin Handbook*; Kadish, K. M., Smith, K. M., Guilard, R., Eds.; Academic Press: Burlington, MA, 2000, Vol. 6, pp 279−340.

 © 2010 American Chemical Society

Scheme 1. Redox Transformation among 16, 18, and 20 π-Electron Porphyrin Cores

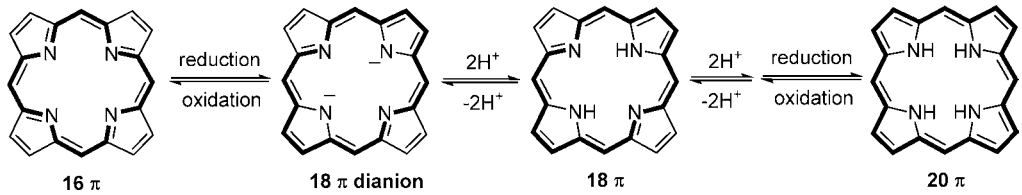

Scheme 2. Synthesis of 16 π-Electron OETPP (**2**) and OiBTPP (**4**)

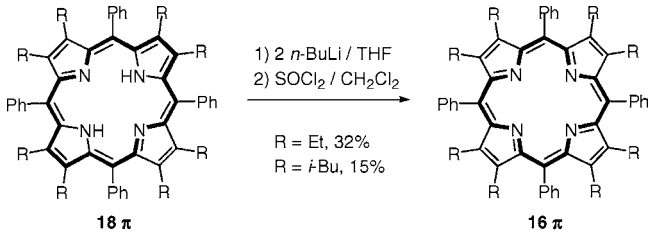

1 (R = Et, $OETPPH_2$)
3 (R = *i*-Bu, $OiBTPPH_2$)

2 (R = Et, OETPP)
4 (R = *i*-Bu, OiBTPP)

electronic structure, the isolation of such "nonaromatic" or "antiaromatic" species is not an easy task, and the pursuit of such species remains a challenge.[2] Thus, for the reduced species (20 π-electron state), *N*,*N*′,*N*″,*N*‴-tetramethylisophlorin,[3a] β-tetrakis(trifluoromethyl)-*meso*-tetraphenylporphyrin,[3b] and tetraphenylporphyrin−silicon[3c] and −germanium complexes[3d] are the only examples that have been isolated and structurally determined. Oxidized porphyrins (16 π-electron state) are even rarer, and only two examples have been reported so far, by us[4] and by Vaid's group,[5] to the best of our knowledge (vide infra).

During the course of our studies to synthesize highly distorted porphyrin−main group element complexes,[6] we fortuitously found that reaction of the dilithiated salt of β-octaethyl-*meso*-tetraphenylporphyrin ($(OETPP)H_2$) or β-octaisobutyl-*meso*-tetraphenylporphyrin ($(OiBTPP)H_2$) with $SOCl_2$ gives doubly oxidized octaalkyltetraphenylporphyrins (OETPP or OiBTPP) with a 16 π-electron core (Scheme 2).[4] X-ray analysis revealed that the 16π porphyrins **2** and **4** were more distorted than the corresponding 18π analogues **1** and **3**, respectively. If a porphyrin core were planar, an aromatic 18π state would be expected to be much more stable than a 16π state. On the other hand, if a porphyrin core were distorted to some extent, the energy difference between the 18π and 16π states would be expected to become smaller due to destabilization of the 18π state. This rationalization implies that the unexpected stability of the 16π state in **2** and **4** arose from the considerable distortion of the porphyrin core caused by the steric bulk of the 12 peripheral substituents. The significance of the deformation of the conjugated core was also supported by the fact that the more distorted OiBTPP (**4**) was more stable than OETPP (**2**). The bond lengths of the porphyrin skeletons in **2** and **4** clearly showed the presence of bond alternation. As shown in Figure 1, there was a unequivocal difference in bond lengths between corresponding adjacent bonds (1.31−1.37 and 1.42−1.49 Å) for 16π OETPP (**2**), suggesting that it was nonaromatic. Another distinct difference between the 16 and 18 π-electron states was observed in the UV−vis spectra. The UV−vis absorptions for 18π $(OETPP)H_2$ (**1**) appeared at 446, 548, and 588 nm, whereas those for 16π OETPP (**2**) were highly blue-shifted to 275 and 339 nm and had smaller extinction coefficients. In addition, no absorptions in the Q-band region were observed for the latter. These experimental results established **2** and **4** as the first fully characterized 16π porphyrins.

After our initial report, Vaid and co-workers disclosed their isolation of $[(TPP)Li]^+[BF_4]^-$ (TPP = *meso*-tetraphenylporphyrin) bearing a 16π porphyrin skeleton by the reaction of dilithiated tetraphenylporphyrin ($Li_2(TPP)$) with thianthrenium tetrafluoroborate ($Thn^+BF_4^-$).[5] This is the only report on the isolation of a 16π porphyrin−metal complex to date. They attempted to remove the lithium cation, but metal-free 16π TPP could not be isolated. Therefore, they concluded that the 16π TPP was probably not stable as a free molecule and required stabilization by coordination to the lithium cation. This is in clear contrast to our sterically distorted **2** and **4**. Nonetheless, the UV−vis spectrum of $[(TPP)Li]^+[BF_4]^-$ (λ_{max} = 332 and 394 nm) was similar to those of **2** and **4**, giving rise to a general trend that the UV−vis spectra of 16π porphyrins show absorptions that are blue-shifted compared with those of their 18π counterparts.

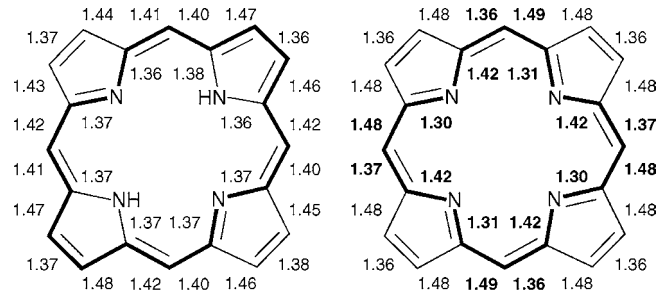

1 ($OETPPH_2$) **2** (OETPP)

Figure 1. Bond alternation in 16 π-electron OETPP (**2**).

(2) (a) Sanders, J. K. M.; Bampos, N.; Clyde-Watson, Z.; Darling, S. L.; Hawley, J. C.; Kim, H.-J.; Mak, C. C.; Webb, S. J. In *The Porphyrin Handbook*; Kadish, K. M., Smith, K. M., Guilard, R., Eds.; Academic Press: Burlington, MA, 2000, Vol. 3, pp 1−48. (b) Kadish, K. M.; Van Caemelbecke, E. Royal, G. In *The Porphyrin Handbook*; Kadish, K. M., Smith, K. M., Guilard, R., Eds.; Academic Press: Burlington, MA, 2000, Vol. 8, pp 1−97. (c) Brothers, P. J. *Adv. Organomet. Chem.* **2001**, *48*, 289–342. (d) Hoard, J. L. In *Porphyrins and Metalloporphyrins*; Smith, K. M., Ed.; Elsevier: Amsterdam, 1975; p 317.

(3) (a) Vogel, E.; Grigat, I.; Köcher, M.; Lex, J. *Angew. Chem., Int. Ed. Engl.* **1989**, *28*, 1655–1657. (b) Liu, C.; Shen, D.-M.; Chen, Q.-Y. *J. Am. Chem. Soc.* **2007**, *129*, 5814–5815. (c) Cissell, J. A.; Vaid, T. P.; Rheingold, A. L. *J. Am. Chem. Soc.* **2005**, *127*, 12212–12213. (d) Cissell, J. A.; Vaid, T. P.; Yap, G. P. A. *J. Am. Chem. Soc.* **2007**, *129*, 7841–7847.

(4) Yamamoto, Y.; Yamamoto, A.; Furuta, S.-y.; Horie, M.; Kodama, M.; Sato, W.; Akiba, K.-y.; Tsuzuki, S.; Uchimaru, T.; Hashizume, D.; Iwasaki, F. *J. Am. Chem. Soc.* **2005**, *127*, 14540–14541.

(5) Cissell, J. A.; Vaid, T. P.; Yap, G. P. A. *Org. Lett.* **2006**, *8*, 2401–2404.

(6) (a) Akiba, K.-y.; Nadano, R.; Satoh, W.; Yamamoto, Y.; Nagase, S.; Ou, Z.; Tan, X.; Kadish, K. M. *Inorg. Chem.* **2001**, *40*, 5553–5567. (b) Yamamoto, Y.; Akiba, K.-y. *J. Organomet. Chem.* **2000**, *611*, 200–209. (c) Yamamoto, A.; Satoh, W.; Yamamoto, Y.; Akiba, K.-y. *Chem. Commun.* **1999**, 147–148. (d) Yamamoto, Y.; Nadano, R.; Itagaki, M.; Akiba, K.-y. *J. Am. Chem. Soc.* **1995**, *117*, 8287–8288.

Scheme 3. Improved Synthesis of 16 π-Electron OiBTPP (**4**) Using $SbCl_5$

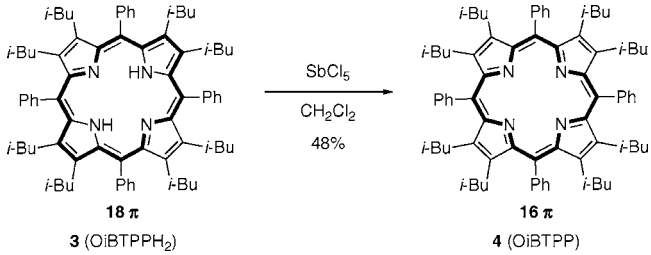

Since the vast majority of known porphyrins are metalloporphyrins, it would be important to reveal the complexation chemistry of 16π porphyrins toward metals. Thus, we decided to examine reactions with metals of varying oxidation levels using OiBTPP (**4**), which is more stable and easier to handle than OETPP (**2**). In this article, we report the details of studies, which culminated in the isolation and structural determination of a 17 π-electron cation radical complex, $[(OiBTPP)Cu]^{\bullet+}[SbF_6]^-$ (**10**), and the first 16 π-electron transition metal complex, $[(OiBTPP)Zn(Cl)]^+[ZnCl_3]^-$ (**11**). Magnetic circular dichroism (MCD) measurements, spectroelectrochemical experiments, and nucleus-independent chemical shift (NICS) calculations were found to be beneficial for elucidation of the electronic properties of the novel porphyrins.

Results and Discussion

Synthesis. First, we needed to improve the final step in the synthesis of **4**, i.e., oxidation of 18π $(OiBTPP)H_2$ (**3**), because the yield of the reaction of $(OiBTPP)Li_2$ with $SOCl_2$ as the oxidant was low (15%) and poorly reproducible (see Scheme 2).[4] Thus, we examined the direct oxidation of **3** with several oxidants (MnO_2, $NOBF_4$, and $SbCl_5$) and found that the reaction using $SbCl_5$ proceeded cleanly to give **4** in moderate yield (48%) with high reproducibility (Scheme 3). $(OETPP)H_2$ (**1**) was also oxidized to give **2** utilizing this method, although the yield was not improved (26%). However, the present method was found to be ineffective for sterically uncrowded planar porphyrins, TPP and β-octaethylporphyrin (OEP). The treatment of $(TPP)H_2$ with $SbCl_5$ resulted in its complete recovery. In the reaction of $(OEP)H_2$, a color change was observed after addition of $SbCl_5$, but the formation of 16π OEP could not be confirmed. These results suggest the effectiveness of using distorted 18π porphyrins for obtaining metal-free 16π porphyrins.

The introduction of metals into **4** using low-valent metal reagents was first examined. Two electronic states could be envisaged for the products of the reaction of **4** with M(*n*) (where *n* is the oxidation number). One was the 16π (OiBTPP)M(*n*) state, where 16π OiBTPP (**4**) just coordinates with the metal with no change in the oxidation states. The other was the 18π (OiBTPP)M($n + 2$) state, which would form upon reduction of **4** with the metal reagent. The redox potential of metals are generally low, and thus, from a thermodynamic viewpoint, products resulting from the latter would be expected. However, if the barrier to electron transfer were large enough, a product from the former might arise. We decided to take our chances on this latter possibility. The reaction of **4** with $Sn^{II}Cl_2$ afforded a tin complex, presumably $(OiBTPP)SnCl_2$, which transformed to $(OiBTPP)Sn(OEt)_2$ (**5**) upon recrystallization from CH_2Cl_2/EtOH (Scheme 4). The UV−vis spectrum of **5** showed an intense Soret-band absorption at 465 nm, together with weak Q-band absorptions at 605 and 657 nm, which is common for

Scheme 4. Reactions of 16 π-Electron OiBTPP (**4**) and $[(OiBTPP)Li]^+[BF_4]^-$ (**6**) with Low-Valent Metal Reagents

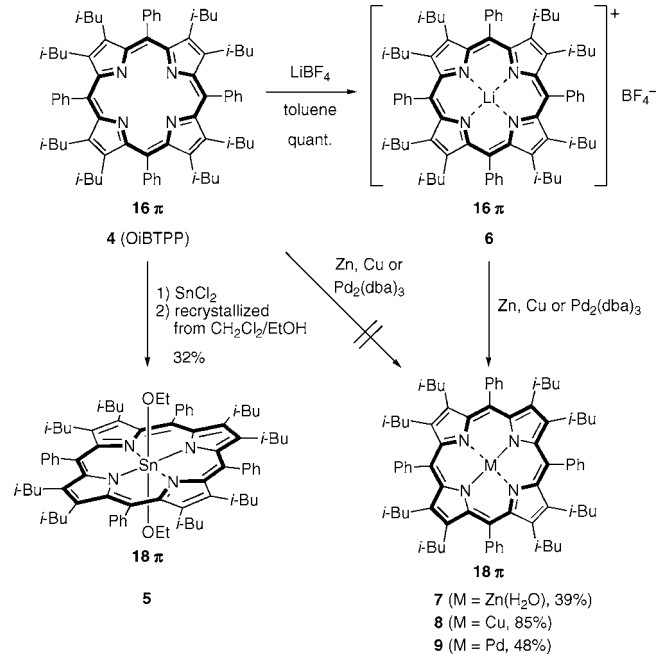

ordinary 18 π-electron porphyrin−metal complexes. Therefore, it was concluded that the reaction of 16π OiBTPP (**4**) with $Sn^{II}Cl_2$ had proceeded in a redox manner; i.e., **4** was reduced to the 18 π-electron state, while the divalent tin atom was oxidized to the tetravalent state.

We next attempted reactions of **4** with zerovalent metals (Mg, Zn, Cu, and $Pd_2(dba)_3$). However, only complex mixtures were obtained, including unidentified 18π and 16π complexes as implicated by UV−vis measurements. Vaid and co-workers disclosed in their study of 16π $[(TPP)Li]^+[BF_4]^-$ that their 16π complex was capable of reacting with Mg, Zn, and Cu to give the corresponding 18π $(TPP)M^{II}$ (M = Mg, Zn and Cu) complexes, respectively.[5] Thus, we examined this methodology for the synthesis of $(OiBTPP)M^{II}$ (M = Zn, Cu, and Pd). The reaction of **4** with $LiBF_4$ in toluene gave $[(OiBTPP)Li]^+[BF_4]^-$ (**6**) quantitatively. Although we could not isolate **6** because of its low stability in air, the formation of **6** could be confirmed by UV−vis spectroscopy (λ_{max} = 365 nm) and ^{7}Li NMR (δ = 1.29 ppm). The reaction of lithium complex **6** with Zn, Cu, and $Pd_2(dba)_3$ afforded 18π porphyrin−metal complexes (OiBTPP)Zn(EtOH) (**7**), (OiBTPP)Cu (**8**), and (OiBTPP)Pd (**9**), respectively (Scheme 4). This result indicates that cationic lithium complex **6** is more favorable for reduction by zerovalent metals than metal-free **4**. The UV−vis spectra of **7**−**9** in CH_2Cl_2 were similar to that of **5**, showing an intense Soret-band absorption (λ_{max} = 476 nm for **7**, 436 nm for **8**, and 440 nm for **9**) and weak broad Q-band absorptions (λ_{max} = 690 nm for **7**, 575 nm for **8**, and 553 and 589 nm for **9**), which again were indicative of the formation of 18 π-electron metalloporphyrins.

The oxidation reaction of copper complex **8** with $AgSbF_6$ resulted in the quantitative formation of the 17 π-electron cation radical complex $[(OiBTPP)Cu]^{\bullet+}[SbF_6]^-$ (**10**) (Scheme 5). The UV−vis spectrum of **10** showed absorptions at 306, 421 (sh), 454, and 623 nm (Figure 2a), and the compound was found to be silent to electron spin resonance (ESR) measurements. These features were quite similar to those reported previously for structurally highly related 17 π-electron cation radical complexes $[(OETPP)Cu]^{\bullet+}X^-$ (X = ClO_4, I).[7b] The lack of an ESR signal

Scheme 5. Oxidation of (OiBTPP)Cu (**8**) by $AgSbF_6$

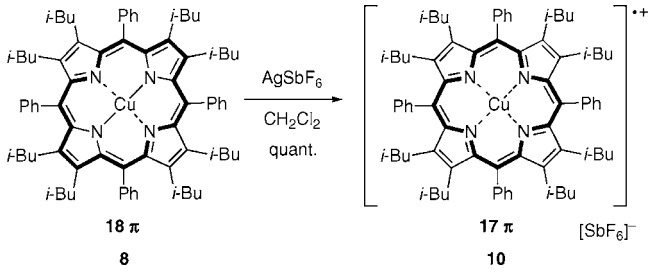

Scheme 6. Reaction of **4** with $ZnCl_2$ to Give 16 π-Electron $[(OiBTPP)Zn(Cl)]^+[ZnCl_3]^-$ (**11**)

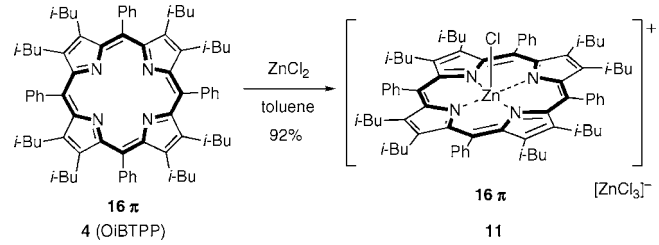

was consistent with the general propensity for coupling between paramagnetic metals such as Cu(II) and nonplanar radical porphyrin ligands to be antiferromagnetic due to effective overlap of the d-orbitals of the metal with the radical π orbitals.[7]

Since the reactions of low-valent and zerovalent metals described in Scheme 4 proceeded in a redox manner to furnish 18π porphyrins, if the reaction proceeded at all, we next examined high-valent metal reagents to avoid reduction of the porphyrin core. No reactions were observed when $NiCl_2$, $MgCl_2$, and $PdCl_2$ were used. However, the reaction of **4** with 2 equiv of $ZnCl_2$ gave 16π zinc complex $[(OiBTPP)Zn(Cl)]^+[ZnCl_3]^-$ (**11**), which was isolated in 92% yield as a brown crystalline solid (Scheme 6). Complex **11** was not very stable in solution but was relatively stable in the solid state. Decomposition leads to what we believe to be products of hydrolysis. However, we have not yet been able to identify them.

The UV−vis spectra of the two zinc complexes **7** and **11** (Figure 2b) were significantly different, with the two major absorptions (340 and 386 nm) of **11** being considerably blue-shifted and having smaller extinction coefficients compared with the Soret-band absorption of **7** (476 nm). In addition, no absorptions were observed in the Q-band region for **11**. This difference is quite similar to that between metal-free analogues **3** and **4**. The absorptions of **11** are more red-shifted than those of metal-free 16π OiBTPP (**4**) (274 and 331 nm) by ca. 60 nm but are comparable to those of $[(TPP)Li]^+[BF_4]^-$ (332 and 394 nm).[5]

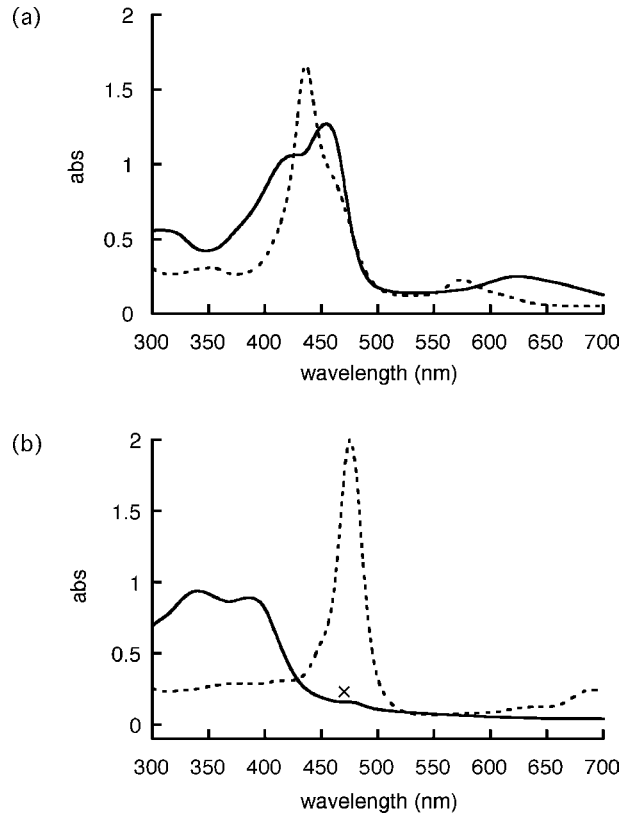

Figure 2. UV−vis spectra of copper and zinc complexes. (a) **8** (c = 12.1 μM; broken line) and **10** (c = 15.3 μM; solid line). (b) **7** (c = 12.2 μM; broken line) and **11** (c = 22.4 μM; solid line) in CH_2Cl_2. The small absorption at 480 nm (marked with a cross) is due to a small amount of a hydrolyzed (18π) species.

Crystal Structure. Single crystals for **5** and **7**−**11** grown from appropriate solvents (ethanol/CH_2Cl_2 for **5**, **7**−**9**; CH_2Cl_2/hexane for **10**; and 1,2-dichloroethane/hexane for **11**) were subjected to X-ray crystallographic analysis. These crystals contained solvent molecules in the crystal lattice (**5**, ethanol; **7**−**9**, CH_2Cl_2; **10**, water;[8] **11**, 1,2-dichloroethane). Figures S1, S2, S4−S6 (see Supporting Information), and 3 show the ORTEP drawings of **5** and **7**−**11**, respectively, and selected structural parameters are summarized in Table 1.

The porphyrin cores of the OiBTPP−metal derivatives are nonplanar. Figure 4 shows the deviation of each atom from the mean plane defined by the 24 core atoms for **5** and **7**−**11**. The core of **5** is distorted only at the β-positions, showing a saddle-type distortion. For **7**−**11**, not only the β-positions but also the *meso*-positions deviate from the mean plane; therefore, these metalloporphyrins take on essentially saddle-type conformations,

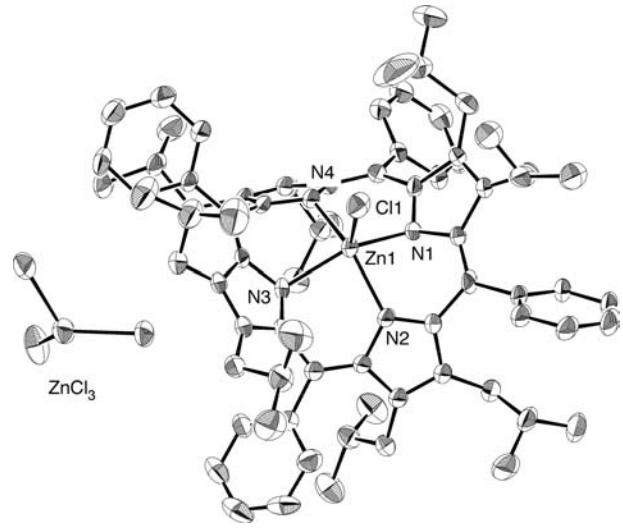

Figure 3. ORTEP drawing of $[(OiBTPP)Zn(Cl)]^+[ZnCl_3]^-$ (**11**) with the thermal ellipsoids shown at the 50% probability level. All hydrogen atoms and solvated molecules are omitted for clarity. Selected bond lengths (Å) and angles (°): Zn1−N1, 2.125(4); Zn1−N2, 2.117(4); Zn1−N3, 2.119(4); Zn1−N4, 2.127(4); Zn1−Cl1, 2.2239(15); N1−Zn1−N2, 83.03(16); N1−Zn1−N3, 142.92(16); N1−Zn1−N4, 84.61(16); N1−Zn1−Cl1, 107.68(12); N2−Zn1−N3, 86.35(16); N2−Zn1−N4, 146.38(17); N2−Zn1−Cl1, 107.82(12); N3−Zn1−N4, 84.94(16), N3−Zn1−Cl1, 109.40(13); N4−Zn1−Cl1, 105.71(12).

Table 1. Selected Structural Parameters for **5** and **7**−**11**

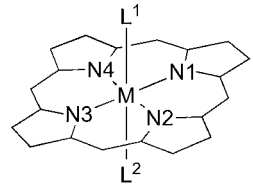

5: M = Sn, $L^1 = L^2$ = OEt
7: M = Zn, L^1 = EtOH, L^2 = none
8: M = Cu, $L^1 = L^2$ = none
9: M = Pd, $L^1 = L^2$ = none
10: M = Cu, $L^1 = L^2$ = none
11: M = Zn, L^1 = Cl, L^2 = none

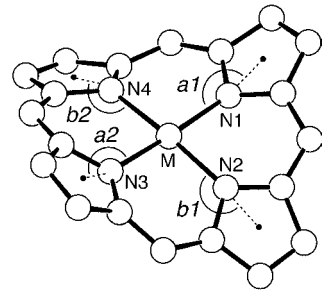

• = the centroid of 5 pyrrole atoms

compound	M−N[a] (Å)	N···N[b] (Å)	M···Δ4N[c] (Å)	a[d] (deg)	b[e] (deg)	RMS[f]	ref
(OiBTPP)Sn(OEt)$_2$ (**5**)	2.1025(16)	4.204(2)	0.000	161.5	161.5	0.502	
(OiBTPP)Zn(EtOH) (**7**)	2.055(3)	4.052(5)	0.338	148.1	167.2	0.641	
(OiBTPP)Cu (**8**)	1.964(2)	3.920(4)	0.010	160.0	160.1	0.690	
(OiBTPP)Pd (**9**)	2.006(4)	4.008(8)	0.005	159.0	159.1	0.671	
[(OiBTPP)Cu]$^{\bullet+}$[SbF_6]$^-$ (**10**)	1.967(3)	3.933(5)	0.001	147.3	147.4	0.821	
[(OiBTPP)Zn(Cl)]$^+$[$ZnCl_3$]$^-$ (**11**)	2.122(4)	4.043(6)	0.643	129.5	149.2	0.888	
OiBTPP (**4**)		4.268(3)				0.921	4
(OETPP)Zn(MeOH)	2.063		0.240			0.669	11
(OETPP)Cu	1.977		0.004			0.700	7b
[(OETPP)Cu]$^{\bullet+}$[ClO_4]$^-$	1.974		0.092			0.838	7b
OETPP (**2**)		4.227(3)				0.836	4

[a] Average value of the four M−N lengths. Standard deviations are in parentheses. [b] Average value of the N1···N3 and N2···N4 distances. Standard deviations are in parentheses. [c] Distance between M and the mean plane consisting of the four nitrogen atoms. [d] Average value of a_1 and a_2. [e] Average value of b_1 and b_2. [f] Root-mean-square of the sum of the squares of the deviation of each atom from the mean plane defined by the 24 core atoms.

with some contribution from ruffle-type distortions. This should be due to considerable crowding at the periphery. Although there is no consistent trend in the orientations of the two isobutyl groups of the pyrrole rings (up−up or up−down), it could be that the isobutyl groups are arrayed to minimize steric repulsions. The degree of overall distortion of the porphyrin core can be evaluated by the root-mean-square of the deviation of each atom from the mean plane (rms value). Among the 18π complexes, the rms value of tin complex **5** is smaller (0.502) than those of the others (0.641 for **7**, 0.690 for **8**, and 0.671 for **9**), indicating that the size of the central metal affects the degree of distortion of the porphyrin core. This agrees with the trend observed for OETPP−metal complexes; i.e., larger metals tend to induce more-planar porphyrin cores.[9] As a result, the transannular N···N distance of **5** (4.20 Å) is longer than those of the others (**7**, 4.05 Å; **8**, 3.92 Å; **9**, 4.01 Å). The rms value for the 17π copper complex **10** (0.821) is much greater than that of the corresponding 18π complex **8** (0.690), as observed for OETPP derivatives ((OETPP)Cu, 0.700; [(OETPP)Cu]$^{\bullet+}$[ClO_4]$^-$, 0.838).[7b] The situation is the same with the two zinc complexes, 18π **7** (0.641) and 16π **11** (0.888), as observed for metal-free OETPPs (**1**, 0.712; **2**, 0.836). These findings establish a structural trend that the lack of aromaticity enhances distortion in the porphyrin core.

The central metals (M) in the metalloporphyrins can be regarded as pseudo-octahedral (for **5**, M = Sn(OEt)$_2$), five-coordinate (for **7**, M = Zn(EtOH); **11**, M = Zn(Cl)), and four-coordinate (for **8**, M = Cu; **9**, M = Pd). The central metals for **5** (Sn), **8** (Cu), and **9** (Pd) are placed essentially in the mean plane defined by the four nitrogen atoms, as shown by the near-zero distance between the central metal atom and the mean plane (M···Δ4N). The M···Δ4N distance for the 17π copper complex **10** is 0.001 Å, whereas that for [(OETPP)Cu]$^{\bullet+}$[ClO_4]$^-$ is reported to be 0.092 Å.[7b] This difference is notable, considering the fact that the only difference in the porphyrin ligand is the identity of peripheral alkyl groups (Et and *i*-Bu). The counteranion ClO_4^- of the latter is located near the Cu atom (the closest Cu···O contact is 2.45 Å), and this proximity is probably the reason for the deviation of the Cu atom toward the axial ClO_4^-. In contrast, for **10**, the anionic counterpart (SbF_6^-) is separated from the Cu atom (the closest Cu···F distance is 5.3 Å), and two solvated water molecules occupy each side of the Cu atom (Cu···O distances are 3.2−3.7 Å). The difference between the two zinc complexes **7** and **11** is remarkable. The M···Δ4N distance of 18π complex **7** (0.338 Å) is slightly larger than that of 18π (OETPP)Zn(MeOH) (0.240 Å),[10] whereas that of 16π complex **11** (0.643 Å) is considerably larger than those of the former two porphyrins. Thus, the coordination of the pyrrole moieties to the metals is skewed due to the distorted porphyrin cores. For the 18 π-electron metalloporphyrins with the "in-plane" metals (**5**, **8**, and **9**), the angles consisting of metal, nitrogen, and the centroid of the pyrrole ring (*a* and *b* in Table 1) are ca. 160°, which deviates from the ideal 180° for coplanarity. The more distorted 17π copper complex **10** (rms = 0.821) shows smaller angles (a = 147.3°, b = 147.4°) than the 18π metalloporphyrins. It is natural that the "out-of-plane" 18π zinc complex **7** shows different

(7) (a) Erler, B. S.; Scholz, W. F.; Lee, Y. J.; Scheidt, W. R.; Reed, C. A. *J. Am. Chem. Soc.* **1987**, *109*, 2644–2652. (b) Renner, M. W.; Barkigia, K. M.; Zhang, Y.; Medforth, C. J.; Smith, K. M.; Fajer, J. *J. Am. Chem. Soc.* **1994**, *116*, 8582–8592.
(8) Crystallizations were performed using undistilled solvents under air.
(9) Sparks, L. D.; Medforth, C. J.; Park, M.-S.; Chamberlain, J. R.; Ondrias, M. R.; Senge, M. O.; Smith, K. M.; Shelnutt, J. A. *J. Am. Chem. Soc.* **1993**, *115*, 581–592.
(10) Barkigia, K. M.; Berber, M. D.; Fajer, J.; Medforth, C. J.; Renner, M. W.; Smith, K. M. *J. Am. Chem. Soc.* **1990**, *112*, 8851–8857.

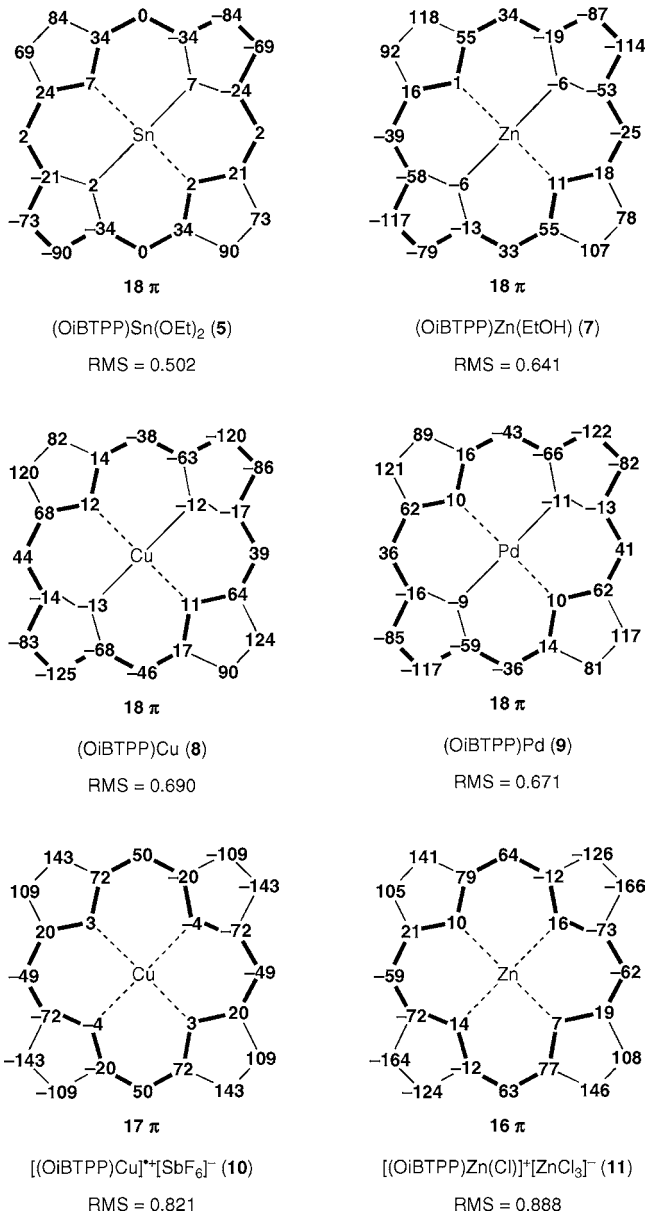

Figure 4. Deviation of each atom from the mean plane (in units of 0.01 Å) in the molecular structure of **5** and **7**−**11** along with rms values (see text).

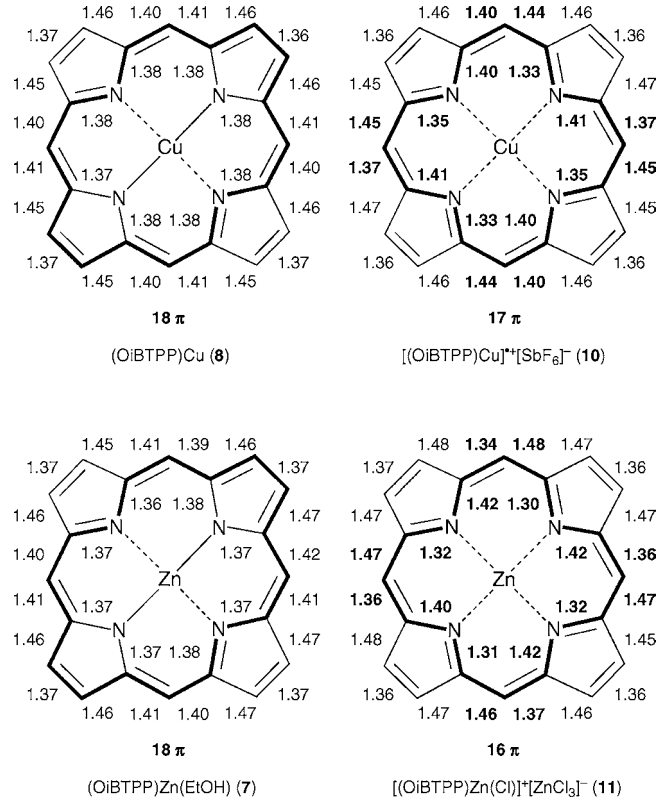

Figure 5. Bond lengths for the porphyrin cores of the copper (**8** and **10**) and zinc (**7** and **11**) complexes.

angles ($a = 148.1°$, $b = 167.2°$). The most distorted complex, **11** (rms = 0.888), shows the smallest *a* angles (average 129.5°: $a_1 = 128.6°$, $a_2 = 130.3°$). This is due to the large M···Δ4N distance (0.643 Å) as well as the large distortion of the core, as shown in Figure S7 (Supporting Information).

Figure 5 shows the bond lengths of the porphyrin cores of the oxidized species (**10** and **11**) and those of the corresponding parent 18π porphyrins (**8** and **7**). Characteristic structural parameters are listed in Table 2, together with those of related compounds. In contrast with aromatic **7** and **8**, unambiguous bond alternations were observed between adjacent C−N bonds ($N-C_{\alpha 1}$ and $N-C_{\alpha 2}$) and between adjacent C−C bonds ($C_m-C_{\alpha 1}$ and $C_m-C_{\alpha 2}$) in the porphyrin cores of the oxidized species **10** and **11**. The average differences between the longer and shorter bond distances are 0.066 ($\Delta(N-C_\alpha)$) and 0.065 Å ($\Delta(C_m-C_\alpha)$) in 17π copper complex **10**, whereas those of 16π zinc complex **11** are 0.101 ($\Delta(N-C_\alpha)$) and 0.114 Å ($\Delta(C_m-C_\alpha)$), indicating that the degree of bond alternation of 16π **11** is larger than that of 17π **10**. The differences in bond lengths of **11** are comparable to those of metal-free 16π porphyrins (**2**, $\Delta(N-C_\alpha) = 0.114$ Å, $\Delta(C_m-C_\alpha) = 0.118$ Å; **4**, $\Delta(N-C_\alpha) = 0.114$ Å, $\Delta(C_m-C_\alpha) = 0.122$ Å) and those of [(TPP)Li][BF_4] ($\Delta(N-C_\alpha) = 0.092$ Å, $\Delta(C_m-C_\alpha) = 0.105$ Å). By carrying out density functional theory (DFT) calculations, Ghosh et al. have recently identified the reason for bond alternations observed for certain π-cation radicals to be pseudo-Jahn−Teller distortion.[11] Through structural optimizations of model zinc−porphine complexes with 16−18 core π-electrons, they have also predicted that the degree of bond alternation of the dicationic zinc complex ($[(P)Zn]^{2+}$) with 16 π-electrons at the core ($\Delta(N-C_\alpha) = 0.0635$ Å, $\Delta(C_m-C_\alpha) = 0.0784$ Å) would be larger than that of the cation radical ($[(P)Zn]^{\bullet+}$) with 17 π-electrons ($\Delta(N-C_\alpha) = 0.0270$ Å, $\Delta(C_m-C_\alpha) = 0.0336$ Å) (Table 2). The trends in the bond lengths of our oxidized metalloporphyrins **10** and **11** are in good agreement with these calculations.

Comparison of the structurally similar $[(OiBTPP)Cu]^{\bullet+}[SbF_6]^-$ (**10**) and $[(OETPP)Cu]^{\bullet+}[ClO_4]^-$ shows that the extent of bond alternation is larger in the former than in the latter (**10**, $\Delta(N-C_\alpha) = 0.066$ Å, $\Delta(C_m-C_\alpha) = 0.065$ Å; $[(OETPP)Cu]^{\bullet+}[ClO_4]^-$, $\Delta(N-C_\alpha) = 0.023$ Å, $\Delta(C_m-C_\alpha) = 0.028$ Å), even though the overall distortions of the porphyrin cores are practically the same (rms = 0.821 and 0.838). This difference is reflected in the deviation of the meso carbon atoms from the mean plane defined by the core atoms (Figure S8, Supporting Information). The average deviation of the meso carbon atoms of **10** (0.050 Å) is much larger than that of $[(OETPP)Cu]^{\bullet+}[ClO_4]^-$ (0.019 Å). It is interesting that the bonding schemes for 17π radicals are sensitive to small changes in the porphyrin ligand (Et and *i*-Bu in the periphery), whereas little difference in the degree of bond alternation is observed among structurally

Table 2. Structural Parameters of the Porphyrin Cores for **7**, **8**, **10**, and **11**[a]

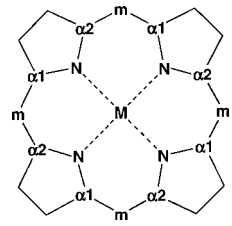

compound	no. of π electrons	average deviation (Å)			average bond distance (Å)[b]				ref
		C_m	$C_{\alpha1}$	$C_{\alpha2}$	$N-C_{\alpha1}$	$N-C_{\alpha2}$	$C_m-C_{\alpha1}$	$C_m-C_{\alpha2}$	
(OiBTPP)Zn(EtOH) (**7**)	18	0.033	0.017	0.055	1.368(6)	1.372(6)	1.411(7)	1.403(6)	
(OiBTPP)Cu (**8**)	18	0.042	0.016	0.066	1.380(4)	1.401(4)	1.405(4)	1.407(4)	
$[(OiBTPP)Cu]^{\bullet+}[SbF_6]^-$ (**10**)	17	0.050	0.020	0.072	1.341(5)	1.407(5)	1.443(6)	1.388(6)	
$[(OiBTPP)Zn(Cl)]^+[ZnCl_3]^-$ (**11**)	16	0.062	0.016	0.075	1.312(6)	1.413(6)	1.472(7)	1.358(7)	
OiBTPP (**4**)	16	0.052	0.020	0.067	1.310(3)	1.424(3)	1.483(4)	1.361(4)	4
$[(OETPP)Cu]^{\bullet+}[ClO_4]^-$	17	0.019	0.038	0.059	1.372(6)	1.395(4)	1.421(6)	1.393(3)	7b
OETPP (**2**)	16	0.060	0.010	0.064	1.306(3)	1.420(3)	1.483(4)	1.365(4)	4
$[(TPP)Li][BF_4]$	16				1.316(3)	1.408(3)	1.470(3)	1.365(3)	5
(P)Zn[c]	18				1.3735	1.3734	1.3977	1.3978	11
$[(P)Zn]^{\bullet+}$ [c]	17				1.3579	1.3849	1.4187	1.3851	11
$[(P)Zn]^{2+}$ [c]	16				1.3395	1.4030	1.4455	1.3671	11

[a] C_m, *meso*-carbon atom; $C_{\alpha1}$, $C_{\alpha2}$; α carbon atoms of the pyrrole ring. [b] Standard deviations are in parentheses. [c] Optimized by DFT calculations carried out under C_{4h} symmetry constraint. P = porphine.

determined 16π species, regardless of the identity of the porphyrin or whether metals are involved.

Harmonic oscillator model of aromaticity (HOMA) values,[12] derived from experimentally determined bond lengths, have been utilized to determine the degree of aromaticity of cyclic conjugated systems, with values close to 1 corresponding to high aromaticity and those close to 0 corresponding to low aromaticity. Calculations based upon this criterion for 17π cation radical complex $[(OiBTPP)Cu]^{\bullet+}[SbF_6]^-$ (**10**) give an average value of 0.451 (0.501 and 0.402), whereas that for the parent (OiBTPP)Cu (**8**) is 0.664 (0.678 and 0.649). As for the 16π dication complex $[(OiBTPP)Zn(Cl)]^+[ZnCl_3]^-$ (**11**), the value is 0.328, whereas the parent (OiBTPP)Zn(EtOH) (**7**) has an average value of 0.603 (0.600 and 0.607). Thus, the two electron-deficient complexes **10** and **11** can be considered to be of low aromaticity, especially **11**.

The crystals of both (OiBTPP)Cu (**8**) and (OiBTPP)Pd (**9**) contain three dichloromethane molecules per porphyrin. These molecules are located close to the porphyrin core, with the distances between the pyrrole nitrogen atom and the carbon atom of dichloromethane being 3.3−3.5 Å, and the hydrogen atoms face the core. There might be C−H···π interactions, as observed for the OETPP···CH_2Cl_2 complex,[4] or it could be that the dichloromethane molecules are simply trapped in the cavity formed by the highly distorted (OiBTPP)M fragments.

Nucleus-Independent Chemical Shift Calculations. The electronic structures of the porphyrins with the 16 and 18 π-electron systems were studied by nucleus-independent chemical shift calculations (NICS). Schleyer et al. proposed NICS as a computational measure of aromaticity that is related to experimental magnetic criteria.[13] NICS is defined as the negative shielding value computed at a ring center or some other points of interest in the system. Rings with negative NICS values are classified as aromatic, while antiaromatic systems have positive values. Indeed, the NICS values at the ring center of aromatic porphyrins have been calculated to be negative.[14]

Table 3. NICS Values (ppm, B3LYP/6-31G*) for Porphyrins and Their Metal Complexes

compound	point a[c]	point b[d]	point c[e]	point d[e]
$(OiBTPP)H_2$ (**3**)[a]	−11.57	−13.45	−1.22	−9.81
OiBTPP (**4**)[a]	+0.53	+2.40	+1.09	+1.00
$(OETPP)H_2$ (**1**)[a]	−12.42	−14.86	−0.61	−10.50
OETPP (**2**)[a]	+0.93	+2.83	+0.41	−0.24
$PorH_2$[a]	−15.25	−18.78	−1.97	−12.73
$PorH_2$[b]	−15.48	−19.26	−2.93	−13.25
Por[b]	+13.20	+19.79	−4.79	−4.79
(OiBTPP)Zn (**7**)[a]		−14.02	−5.03	−5.68
$[(OiBTPP)Zn(Cl)]^+$ (**11**)[a]		+4.38	+0.42	−0.50
PorZn[b]		−18.00	−8.28	−8.28
$[PorZnCl]^+$ [b]		+35.09	−4.00	−3.98
(OiBTPP)Cu (**8**)[a]		−15.38	−5.09	−5.15
$[(OiBTPP)Cu]^+$ (**10**)[a]		−13.09	−5.86	−6.22
PorCu[b]		−19.82	−7.97	−7.98
$[PorCu]^+$ [b]		−3.49	−10.61	−10.62

[a] X-ray geometry. OETPP, 2,3,7,8,12,13,17,18-octaethyl-5,10,15,20-tetraphenylporphyrin;[4] $PorH_2$ = free-base porphine.[15] [b] Optimized structure calculated at the level of B3LYP/6-31G*. Por, porphine. [c] Value at the center of the inner 16-membered ring. [d] Average of the values at the midpoint of two C−N bonds. [e] Average of the values at the center of two pyrrole rings.

As shown in Table 3 and Figure 6, NICS values were calculated for the X-ray geometries of the present porphyrins at the center of the inner 16-membered ring (point a), the midpoint of two C−N bonds (point b), and the centers of two inequivalent pyrrole rings (points c and d). We have also calculated NICS indices at these points for the optimized structures of free-base and metal porphines (porphyrins without peripheral substituents) to probe the effect of the peripheral substitution on the NICS values. Unfortunately, full structural

(11) Vangberg, T.; Lie, R.; Ghosh, A. *J. Am. Chem. Soc.* **2002**, *124*, 8122–8130.
(12) Krygowski, T. M. *J. Chem. Inf. Comput. Sci.* **1993**, *33*, 70–78. For aromatic porphyrin systems, the value may change depending on how the 18 bonds are selected. Therefore, the two values are shown in parentheses with the average of the two outside of it.
(13) Schleyer, P. v. R.; Meaerker, C.; Dransfeld, A.; Jiao, H.; Hommes, N. J. R. v. E. *J. Am. Chem. Soc.* **1996**, *118*, 6317–6318.
(14) Cyrañski, M. K.; Krygowski, T. M.; Wisiorowski, M.; Hommes, N. J. R. v. E.; Schleyer, P. v. R. *Angew. Chem., Int. Ed.* **1998**, *37*, 177–180.

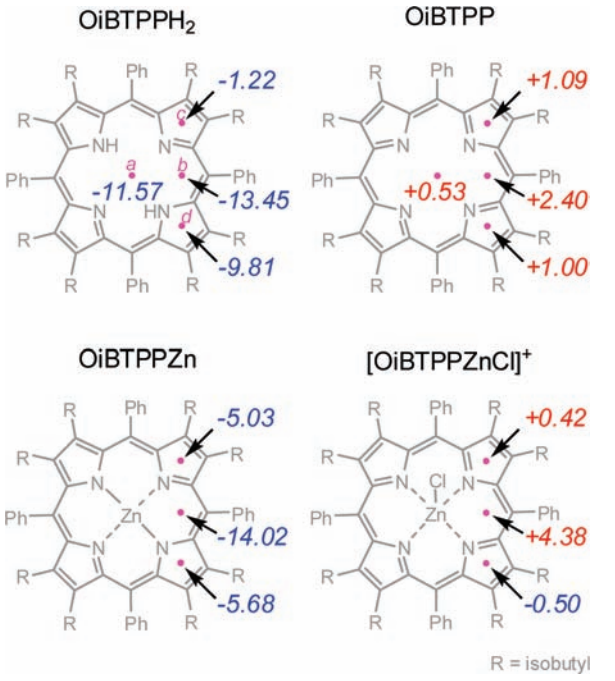

Figure 6. NICS values (ppm) calculated for free-base and Zn porphyrins (B3LYP/6-31G*).

optimization of the actual complexes with multiple peripheral substituents could not be carried out. The reliability of our analysis could be confirmed by the good agreement between NICS values for the experimentally reported[15] and theoretically optimized $PorH_2$. As would be expected, the DFT-optimized porphines adopt a more planar structure than the corresponding X-ray geometries (see Figure S9, Supporting Information).

In the case of 18π free-base porphyrin ($(OiBTPP)H_2$, **3**), the NICS values at points a and b were calculated to be −11.57 and −13.45, respectively, which are comparable with those reported for aromatic porphyrins.[14] On the other hand, OiBTPP (**4**) exhibits markedly different NICS signatures. The values at points a and b are positive but small in magnitude (+0.53 at point a, +2.40 at point b), indicating the ring current to be weakly paratropic. Similar positive NICS values were calculated at points a and b for the X-ray geometry of OETPP (**2**). The NICS values of +13.20 and +19.79 at points a and b for the 16π porphine (Por) indicate the ring current to be strongly paratropic (see Table 3). Thus, the highly antiaromatic nature of Por implied by the NICS values compared with those of OiBTPP may be a consequence of the planarity of the porphyrin skeleton in Por. The NICS values at points c and d for OiBTPP were also different from those for Por.

The oxidized form of the zinc complex, $[(OiBTPP)Zn(Cl)]^+$ (**11**), has a positive NICS value at point b (+4.38). The NICS calculation for $[PorZn]^+$ indicates a more positive value at point b (+35.09), which is almost the same as that for $[LiPor]^+$ (+36.5) reported by Vaid et al.[5] These results confirm that the electronic structure of $[(OiBTPP)Zn(Cl)]^+$ can be described as a nonaromatic 16 π-electron system with only weak paratropic ring current. The difference between the NICS signs at points c (+0.42) and d (−0.50) is likely due to distortion of planarity, as observed for the X-ray structure. The calculated NICS values were essentially the same, even when other basis sets (6-311G*, SVP, and LanL2DZ) were used for the zinc atom instead of the 6-31G* basis set. Thus, the effect of the basis set on the NICS values should not be important (see Table S2, Supporting Information).

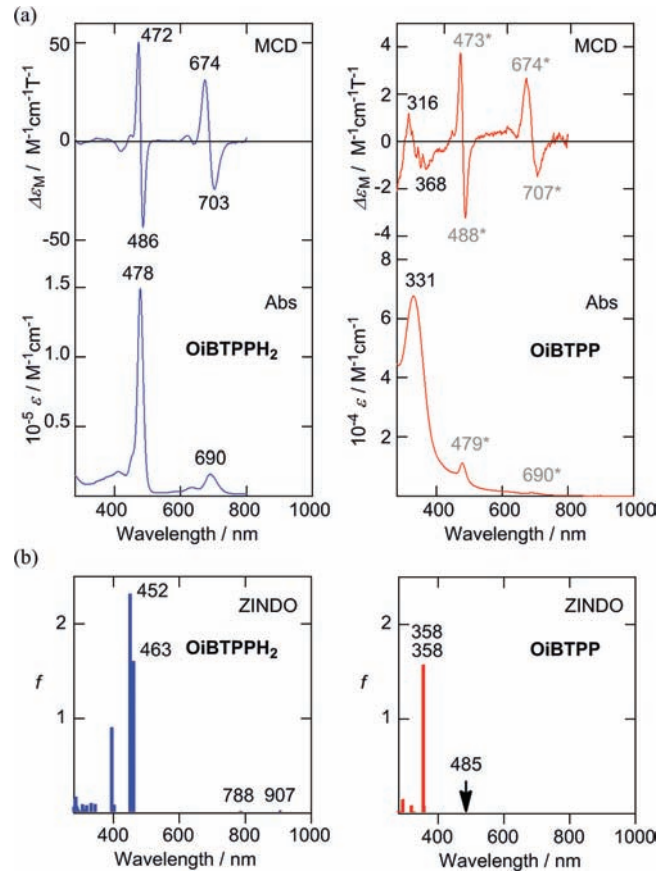

Figure 7. (a) MCD and electronic absorption spectra of $(OiBTPP)H_2$ (**3**, left) and OiBTPP (**4**, right) measured in CH_2Cl_2. Bands marked with asterisks are due to trace amounts of products of decomposition. (b) Calculated absorption spectra of the free-base porphyrins obtained using the ZINDO/S method.

We have also calculated NICS values for the two forms (17 and 18π) of copper porphyrins. The NICS value at point b for $[(OiBTPP)Cu]^{\bullet+}$ (**10**) remains negative upon oxidation, implying that the singly oxidized form of the Cu complex more or less has aromatic character.

Magnetic Circular Dichroism Spectra and MO Analysis. MCD spectroscopy has been one of the most powerful techniques for analyzing the electronic excited states of aromatic porphyrins and related macrocyclic systems derived from an 18 π-electron core.[16] Very recently, a subgroup of the authors demonstrated that the electronic absorption spectra of expanded porphyrins with a [4n] π-electron system can also be characterized using MCD techniques.[17] Here we report the first MCD spectra for the 16 π-electron porphyrins and rationalize the spectral changes upon oxidation on the basis of ZINDO/S calculations and molecular orbital analyses.

Figure 7a shows the UV−vis and MCD spectra of the two forms (16 and 18π) of free-base porphyrin (**3** and **4**) in CH_2Cl_2.

(15) Saltsman, I.; Goldberg, I.; Balasz, Y.; Gross, Z. *Tetrahedron Lett.* **2007**, *48*, 239–244.

(16) (a) Mack, J.; Stillman, M. J.; Kobayashi, N. *Coord. Chem. Rev.* **2007**, *251*, 429–453. (b) Kobayashi, N.; Nakai, K. *Chem. Commun.* **2007**, 4077–4092.

(17) (a) Sankar, J.; et al. *J. Am. Chem. Soc.* **2008**, *130*, 13568–13579. (b) Muranaka, A.; Matsushita, O.; Yoshida, K.; Mori, S.; Suzuki, M.; Furuyama, T.; Uchiyama, M.; Osuka, A.; Kobayashi, N. *Chem.—Eur. J.* **2009**, *15*, 3744–3751.

Table 4. Selected Results of ZINDO/S Calculations for Low-Energy $\pi-\pi^*$ Transitions of 18 and 16 π-Electron Porphyrins

compound	λ (nm)	f	composition (weight, %)[a]
$(OiBTPP)H_2$ (**3**)	907	0.023	H→L (39.9), H−1→L+1 (24.7), H→L+1 (15.7), H−1→L (14.4)
	788	0.014	H−1→L (33.5), H→L+1 (31.8), H→L (20.1), H−1→L+1 (10.4)
	463	1.601	H−1→L+1 (42.6), H→L (22.8), H−3→L (14.7)
	452	2.312	H→L+1 (40.9), H−1→L (39.2)
OiBTPP (**4**)	485	0.000	H→L [$s_-\rightarrow s_+$][b] (81.3)
	358	1.570	H→L+1 [$s_-\rightarrow l_-$][b] (56.2), H−1→L [$h_+\rightarrow s_+$][b] (18.7)
	358	1.570	H→L+2 [$s_-\rightarrow l_+$][b] (56.4), H−2→L [$h_-\rightarrow s_+$][b] (18.7)

[a] H = HOMO; L = LUMO. [b] Perimeter labels.

A derivative-shaped MCD signal with a negative/positive sign sequence, with increasing energy, was observed for the Q_{00} band of $(OiBTPP)H_2$ (**3**). This type of MCD signal is called an apparent Faraday *A* term and arises from an electronic transition to nearly degenerate excited states.[18] The spectral appearance of **3** is similar to that of $[(OEP)H_4]^{2+}$, which adopts a saddle geometry. Although large signals derived from traces of **3** were observed in the visible region for OiBTPP (**4**), a distinctive derivative-shaped MCD signal with a negative/positive sign sequence for **4** could be detected in the UV region. Because **4** has S_4 symmetry in the X-ray structure, the MCD signal should be assigned to a positive Faraday *A* term, which arises from transitions involving degenerate excited states.

Transition energies and oscillator strengths for the X-ray geometries of these porphyrins were calculated using the ZINDO/S method (Table 4). As can be seen from Figure 7b, the profiles of the calculated absorption spectra of both porphyrins are in close agreement with the observed spectral pattern. A doubly degenerate UV transition (358 nm) was deduced for OiBTPP (**4**), which is in accordance with the observed MCD *A* term. The calculations also predict that a dipole-forbidden HOMO→LUMO transition is located at 485 nm. The observed absorption shoulder that extends to about 800 nm is therefore associated with this HOMO→LUMO transition. This type of forbidden transition is characteristic of cyclic [4*n*] π-electron systems.[17b,19]

Figure 8 shows the energy levels of key frontier π-orbitals and their contour plots for the neutral and oxidized porphyrins. It is evident that the nodal patterns of the frontier orbitals of OiBTPP (**4**) are derived from those of $(OiBTPP)H_2$ (**3**). The four orbitals play an essential role in the low-energy electronic transitions of **3** and **4** (see Table 4). In the case of the 16π porphyrin, two additional occupied orbitals also contribute to the 358 nm transition, and these six orbitals can be labeled as h_-, h_+, s_-, s_+, l_-, and l_+ according to the 4*n*-electron perimeter

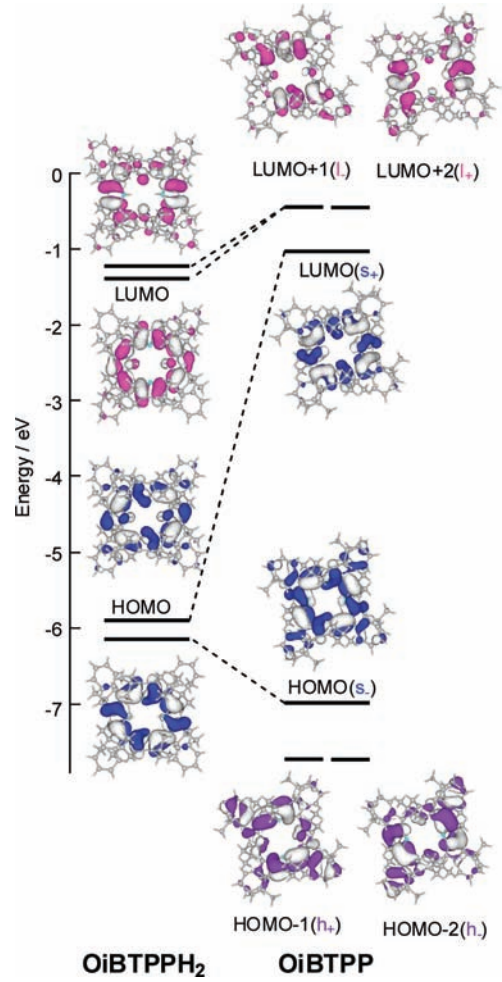

Figure 8. Energy levels of key molecular orbitals and their contour plots for $(OiBTPP)H_2$ (**3**, left) and OiBTPP (**4**, right). The values were obtained from the ZINDO/S calculations for the X-ray geometries. Perimeter labels are given in parentheses.

model.[20] Because the HOMO→LUMO ($s_-\rightarrow s_+$) transition is of intrashell nature in the perimeter model, the transition is magnetic-dipole allowed, but the absorption and MCD intensities are predicted to be zero.

The experimental and calculated spectra of the zinc complexes are given in Figure S10 (Supporting Information). The oxidized zinc complex (**11**) exhibits two distinct absorption bands in the UV region and a broad shoulder in the visible region. The MCD signals corresponding to the two UV absorption bands have negative and positive signs, so these signals are assigned to coupled Faraday *B* terms, which arise from magnetically induced mixing of nondegenerate excited states. The calculated spectral features for both zinc complexes reproduced the experimental spectra well. The split UV transitions for **11** can be derived from the loss of orbital degeneracy, because the insertion of zinc lowers the four-fold symmetry (Figure S11, Supporting Information). The nodal patterns for key frontier molecular orbitals of the zinc complexes are quite similar to those of the free-base porphyrins.

Electrochemistry and Spectroelectrochemistry. The redox properties of $(OiBTPP)H_2$ (**3**) and OiBTPP (**4**) were examined

(18) Mack, J.; Asano, Y.; Kobayashi, N.; Stillman, M. J. *J. Am. Chem. Soc.* **2005**, *127*, 17697–17711.
(19) (a) Fleischhauer, J.; Höweler, U.; Spanget-Larsen, J.; Raabe, G.; Michl, J. *J. Phys. Chem. A* **2004**, *108*, 3225–3234. (b) Fleischhauer, J.; Raabe, G.; Klingensmitj, K. A.; Höweler, U.; Chatterjee, R. K.; Hafner, K.; Vogel, E.; Michl, J. *Int. J. Quantum Chem.* **2005**, *102*, 925–939.
(20) (a) Fleischhauer, J.; Höweler, U.; Michl, J. *J. Chem. Soc., Perkin Trans. 2* **1998**, 1101–1117. (b) Fleischhauer, J.; Höweler, U.; Michl, J. *Spectrochim. Acta* **1999**, *55A*, 585–606. (c) Fleischhauer, J.; Höweler, U.; Michl, J. *J. Phys. Chem. A* **2000**, *104*, 7762–7775.

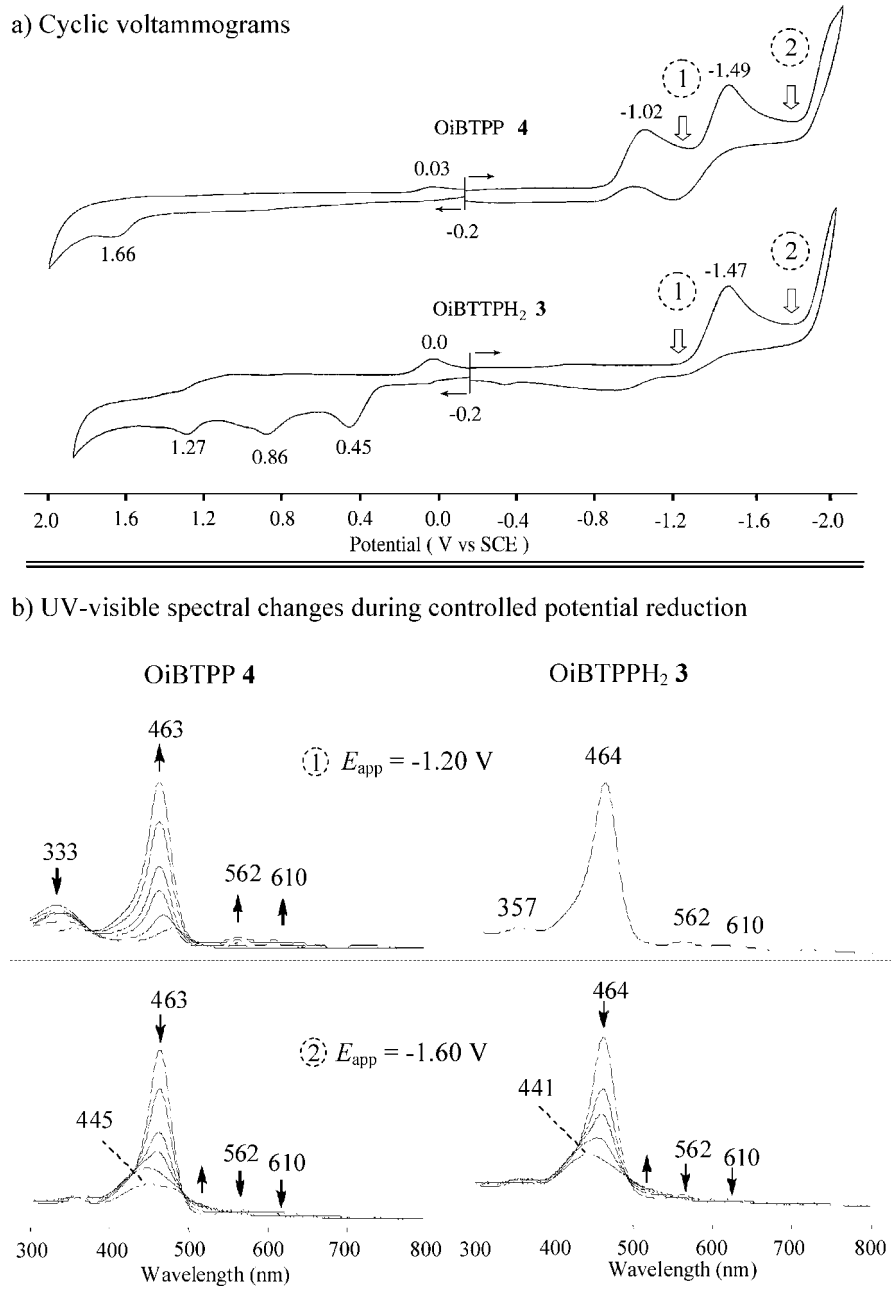

Figure 9. (a) Cyclic voltammograms of OiBTPP (**4**) and $(OiBTPP)H_2$ (**3**) in CH_2Cl_2 containing 0.1 M TBAP at a scan rate of 0.1 V/s. (b) Thin-layer UV−visible spectral changes during controlled potential reduction at (1) −1.20 V and (2) −1.60 V in CH_2Cl_2 containing 0.1 M TBAP.

Table 5. Half-Wave ($E_{1/2}$) and Peak (E_p) Potentials (V vs SEC) in CH_2Cl_2 Containing 0.1 M TBAP

compound	oxidation				reduction			Δ (V)[c]
OiBTPP (**4**)	1.66[a]				−1.02[a]	−1.49[a]	−1.99[a]	0.50
$(OiBTPP)H_2$ (**3**)		1.27[a]	0.86[a]	0.45[a]		−1.47[a]	−1.99[a]	0.52
$(OEP)H_2$[b]		1.40	0.89			−1.44	−1.90	0.46

[a] Peak potential at a scan rate of 0.1 V/s. [b] Data taken from ref 22. [c] Potential difference between the last two processes.

in CH_2Cl_2 containing 0.1 M TBAP. Examples of cyclic voltammograms in CH_2Cl_2 are shown in Figure 9a, while a summary of redox potentials is given in Table 5, which includes data for the related $(OEP)H_2$ derivative. This latter compound exhibits reversible one-electron oxidations and reductions in CH_2Cl_2, leading to a π-cation radical (17π), dication (16π), π-anion radical (19π), and dianion (20π), respectively.[21]

The difference in potentials between the two porphyrin ring-centered reductions of $(OEP)H_2$ is 0.46 V, compared to 0.52 V for $(OiBTPP)H_2$ (**3**). A similar separation of 0.50 V is also seen between the second and third reductions of OiBTPP (**4**). This compound undergoes an irreversible reduction at $E_p = -1.02$ V prior to two additional processes at $E_p = -1.49$ and -1.99 V in CH_2Cl_2. The latter potentials are virtually identical to the E_p values for the two reductions of **3** (see Table 5), suggesting an

(21) (a) Kadish, K. M. *Prog. Inorg. Chem.* **1986**, *34*, 435–605. (b) Kadish, K. M.; Caemelbecke, V.; E.; Royal, G. In *The Porphyrin Handbook*; Kadish, K. M., Smith, K. M., Guilard, R., Eds.; Academic Press: San Diego, CA, 2000; Vol. 8, pp 1−97. (c) Kadish, K. M.; Royal, G.; Caemelbecke, V. E.; Gueletti, E. In *The Porphyrin Handbook*; Kadish, K. M., Smith, K. M., Guilard, R., Eds.; Academic Press: San Diego, CA, 2000; Vol. 9, pp 222−413.
(22) Stolzenberg, A. M.; Spreer, L. O.; Holm, R. H. *J. Am. Chem. Soc.* **1980**, *102*, 364–370.

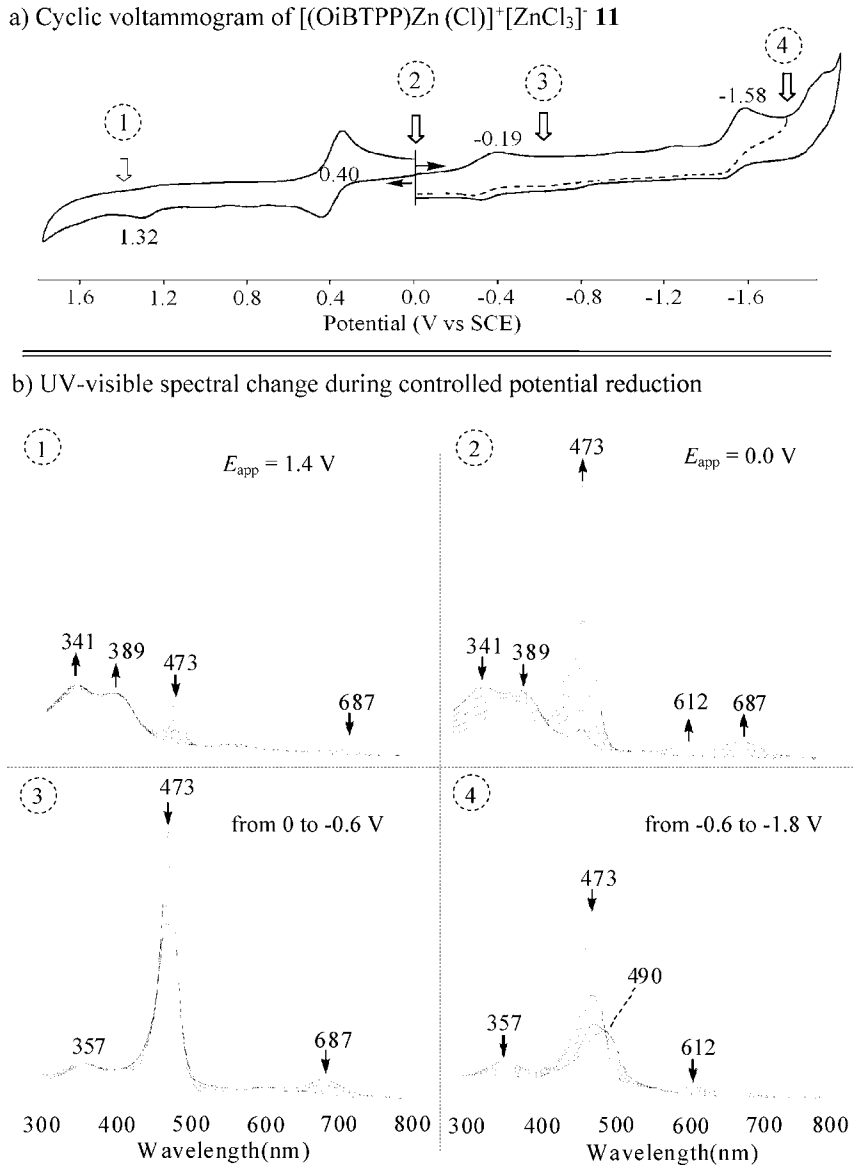

Figure 10. (a) Cyclic voltammograms of $[(OiBTPP)Zn(Cl)]^+[ZnCl_3]^-$ (**11**) in PhCN containing 0.1 M TBAP. (b) UV−visible spectral changes during controlled potential reduction at the indicated potentials.

electrochemical conversion of **4** to **3** under the given solution conditions. The reduction at −1.02 V is irreversible and involves an overall two-electron, two-proton addition, where the protons come from the solvent or supporting electrolyte.

More definitive evidence for the electrochemically initiated conversion of OiBTPP (**4**) to $(OiBTPP)H_2$ (**3**) is given by the thin-layer spectroelectrochemical data. A CH_2Cl_2 solution of **3** exhibits absorption bands at 357, 464, 526, and 610 nm (Figure 9b, top right), and exactly the same spectral pattern is observed for the product formed after controlled potential reduction of **4** at −1.20 V in the thin-layer cell (Figure 9b, top left). Further controlled potential reduction of the electroreduced **4** solution as well as $(OiBTPP)H_2$ (**3**) at −1.60 V gave in both cases identical spectral products, assigned to the porphyrin π-anion radical of **3**. These spectra are characterized by a broad band at 441−445 nm, and the spectral transitions during reduction are shown in the bottom of Figure 9b. The conversion of **4** to **3** does not occur in a single two-electron, two-proton step but rather involves one or more chemical reactions following an initial electron transfer, after which the second electron is added on longer time scales (see Figure S12, Supporting Information). This is also demonstrated by a reduced peak current for the process at −1.02 V whose shape is consistent with an EC-type mechanism (electron transfer followed by a chemical reaction) where one electron is transferred in the initial step.

The electrochemical oxidation of free-base porphyrins is often complicated in nonaqueous media due to the presence of coupled chemical reactions.[21b,c,23] This is also the case for $(OiBTPP)H_2$ (**3**), which undergoes three irreversible oxidations, as shown in Figure 9a. Attempts were made to electrochemically convert **3** to **4** by oxidation in CH_2Cl_2, but this did not occur, leading instead to a mixture of protonated products as was reported for $(OEP)H_2$ and $(TPP)H_2$.[23]

The electrochemistry of $[(OiBTPP)Zn(Cl)]^+[ZnCl_3]^-$ (**11**) was also investigated, and the spectra of the oxidation and reduction products were elucidated by thin-layer UV−vis spectroelectrochemistry. These studies were carried out in PhCN, where a

(23) Inisan, C.; Saillard, J.-Y.; Guilard, R.; Tabardc, A.; Mest, Y. L. *New J. Chem.* **1998**, 823–830.

well-defined reversible reduction to the 18π porphyrin is observed at $E_{1/2} = 0.40$ V vs SCE. The cyclic voltammogram of **11** in PhCN, 0.1 M TBAP is shown in Figure 10a, and the spectral changes obtained during application of selected applied potentials between +1.4 and −1.8 V are illustrated in Figure 10b.

[(OiBTPP)Zn(Cl)]$^+$[$ZnCl_3$]$^-$ (**11**) initially exhibits absorptions of 341 and 389 nm associated with the pure 16π compound as well as an additional band at 473 nm which was earlier assigned as a small amount of reduced 18π species (see Figures 2 and 10b). The 18π porphyrin was first electrochemically removed from solution by oxidation at 1.40 V, and this was accompanied by a disappearance of the bands at 473 and 687 nm, indicating conversion to a pure oxidation state of the compound (see Figure 10b, top left). The applied potential was then set at 0.0 V, which led to a rapid loss of the bands at 341 and 389 nm and the appearance of an 18π porphyrin-like spectrum having an intense Soret band at 473 nm and two Q-bands at 612 and 687 nm. These spectral changes are shown in the top right of Figure 10b, and the final spectrum after reduction is virtually identical to the spectrum of compound **7** illustrated in Figure 2b. Further reduction of **11** at −0.60 and then −1.80 V led to a marked decrease in the Soret band intensity, suggesting formation of a porphyrin π-anion radical.[24]

To summarize the electrochemical studies, [(OiBTPP)-Zn(Cl)]$^+$[$ZnCl_3$]$^-$ (**11**) undergoes two major redox processes in PhCN. The first, at 0.40 V, involves conversion of the 16π compound to its 18π porphyrin form, most likely (OiBTTP)Zn, and the second, at −1.58 V, involves the expected conversion of the porphyrin to its π-anion radical form. The reduction potentials for porphyrins with OETPP and related macrocycles are quite similar to those of the OEP derivatives with the same center metal ion,[20b,c] and this is also case for **11**, whose E_p value of −1.58 V compares well with the $E_{1/2} = -1.64$ V for reduction of (OEP)Zn under the same solution conditions. A similar reduction of **11** to its 18π porphyrin form occurs in CH_2Cl_2, with the product of the reduction being characterized by a Soret band at 470 nm and two Q-bands at 595 and 681 nm. A further reduction of the compound to give the Zn(II) porphyrin π-anion radical occurs at $E_{1/2} = -1.64$ V in CH_2Cl_2.

Conclusion

We have investigated the reaction of 16π OiBTPP (**4**) with a variety of metal reagents. Using zerovalent metal reagents (Zn, Cu, $Pd_2(dba)_3$), no reaction took place. However, the redox reaction of **4** with $SnCl_2$ followed by ethanolysis afforded 18π (OiBTPP)Sn(OEt)$_2$ (**5**). The 18π metal complexes (OiBTPP)M (M = Zn(EtOH)(**7**), Cu (**8**), and Pd (**9**)) were successfully synthesized by the reaction of 16π lithium complex [(OiBTPP)Li]$^+$[BF_4]$^-$ (**6**) with Zn, Cu, and $Pd_2(dba)_3$, respectively. One-electron oxidation of copper complex **8** by $AgSbF_6$ afforded a 17 π-electron cation radical complex, [(OiBTPP)-Cu]$^{\bullet+}$[SbF_6]$^-$ (**10**). The reaction of **4** with $ZnCl_2$ afforded a novel 16π zinc complex, [(OiBTPP)Zn(Cl)]$^+$[$ZnCl_3$]$^-$ (**11**). The identities of the metalloporphyrins were confirmed by single-crystal X-ray analysis and UV−vis spectroscopy. X-ray analysis of the oxidized species **10** and **11** revealed the presence of distinctive bond alternations, suggestive of the nonaromatic nature of **10** and **11**. The degree of bond alternation in **11** was undoubtedly greater than that in **10**. The essentially nonaromatic and only weakly antiaromatic nature of the 16π porphyrins was confirmed by NICS calculations. The combination of MCD studies and MO (ZINDO/S) analyses unambiguously explained the characteristic features of the UV−vis spectra of the 16π porphyrins. Electrochemical studies of OiBTPP (16π **4**) and [(OiBTPP)Zn(Cl)]$^+$[$ZnCl_3$]$^-$ (16π **11**) indicated that **4** could be reduced to its 18π porphyrin form in CH_2Cl_2 and **11** was capable of undergoing the same transition in CH_2Cl_2 or PhCN. The 16π/18π transition of **11** was reversible in PhCN, and further reduction of the 18π compound occurred at $E_{1/2}$ values quite similar to those for the reduction of (OEP)Zn to its π-anion radical form in the same two solvents. The UV−vis spectrum of electroreduced **11** was virtually identical to that of (OiBT-TP)Zn(EtOH) **7**, thus confirming the assignment of the 16π-to-18π electrochemical conversion. The examination of other porphyrin systems for the preparation of other novel 16π complexes is currently in progress.

Acknowledgment. We are grateful to the RIKEN Super Combined Cluster (RSCC) for computational resources. This work was supported by two Grants-in-Aid for Scientific Research on Priority Areas (Nos. 14340199, 17350021) from the Ministry of Education, Culture, Sports, Science and Technology, Japan, and the Robert A. Welch Foundation (K.M.K., Grant E-680).

Supporting Information Available: Complete ref 17a, experimental details, calculated structures of some porphyrins, and CIF files for **3**, **5**, and **7**−**11**. This material is available free of charge via the Internet at http://pubs.acs.org.

JA102817A

(24) (a) Perrin, M. H.; Gouterman, M.; Perrin, C. L. *J. Chem. Phys.* **1969**, *50*, 4137–4151. (b) Fuhrhop, J. H. *Struct. Bonding (Berlin)* **1974**, *18*, 1–67. (c) Gouterman, M. *J. Mol. Spectrosc.* **1961**, *6*, 138–163.